Intense Ground-Level Enhancements of Solar Cosmic Rays During the Last Solar Cycles

**M. Andriopoulou · H. Mavromichalaki · C. Plainaki ·
A. Belov · E. Eroshenko**

Abstract Ground-level enhancements of solar cosmic rays are sharp increases of short duration in the counting rates of ground-based neutron monitors. Their study is of particular importance, mainly due to their involvement in a vast range of applications such as the prediction of particle fluxes that may be harmful for satellite systems and telecommunication, the analysis of the interplanetary conditions, and the prediction of strong geomagnetic storms. In this work, we make a statistical analysis of the ground-level enhancements events occurring during solar Cycles 22 and 23, in an effort to reveal their common properties and possible physical mechanisms. Data of one- and five-minute resolutions are used, obtained from the worldwide network of neutron monitors and from the high-resolution NMDB database. The analysis includes onset-time calculations, determination of the maximum cosmic ray intensity, and determination of the longitudinal and latitudinal distribution. Moreover, a brief description of the most intense events is given. Finally, the importance of such a statistical analysis in space weather studies is discussed.

Keywords Cosmic rays · Solar energetic particles · Neutron monitors

1. Introduction

Solar energetic particles (SEPs) are highly energetic particles that are occasionally emitted from the Sun and seem to be associated either with solar flares (SFs) and/or with Coronal Mass Ejections (CMEs). Solar energetic particle events with energy greater than 500 MeV

M. Andriopoulou (✉) · H. Mavromichalaki · C. Plainaki
Physics Department, University of Athens, Athens, Greece
e-mail: mariand@phys.uoa.gr

C. Plainaki
IFSI-Istituto di Fisica dello Spazio Interplanetario, Rome, Italy

A. Belov · E. Eroshenko
IZMIRAN Russian Academy of Sciences after Puskov, Moscow, Russia

Springer

are also known as Ground-level Enhancements (GLEs) of solar cosmic rays, since their energetic particles have high enough energies in order to penetrate inside the Earth's atmosphere and finally to be recorded by ground-based neutron monitors (NMs) (Simpson, 2000). Since their official registration, which began in 1942, 70 GLEs have been recorded from the worldwide network of neutron monitors. The first GLE was registered on 28 February 1942 and it was named GLE01 and the most recent one was the GLE70, which was recorded on 13 December 2006 (Plainaki *et al.*, 2009a). The most intense event occurred on 28 February 1956 (GLE05) (Belov *et al.*, 2005a, 2005b), while several tens of recent works have been devoted to GLE69 of 20 January 2005 (Belov *et al.*, 2005c; Vashenyuk *et al.*, 2006; Plainaki *et al.*, 2007).

The study of ground-level enhancements is of particular importance, mainly due to their involvement in a vast range of applications such as the prediction of particle fluxes that may be harmful for satellite systems and telecommunication (Dorman *et al.*, 2003; Mavromichalaki *et al.*, 2007), the analysis of interplanetary conditions (Flückiger *et al.*, 2006), and the prediction of strong geomagnetic storms (Wang and Wang, 2006). Therefore, several techniques, including the analysis and the modeling of GLE characteristics, have been presented in the past (Smart, Shea, and Taskanen, 1971; Shea and Smart, 1982; Humble *et al.*, 1991; Cramp *et al.*, 1997; Belov *et al.*, 2005a; Plainaki *et al.*, 2007 *etc.*). Along the same lines, a general GLE-alert system using real-time data from 23 neutron monitors has recently been developed in the Athens neutron-monitor station (Mavromichalaki *et al.*, 2007, 2010; Souvatzoglou *et al.*, 2009). This system has the ability to provide the earliest alert possible for a SEP event onset, while it tries to minimize the possibility of a false alarm at the same time (see http://cosray.phys.uoa.gr for further information). In order to provide a successful, accurate, and reliable warning system of GLE events, a detailed study of their main properties is necessary.

Although analytical studies have shown that each ground-level enhancement constitutes a unique case characterized by the specific solar and interplanetary conditions during the time period that the event took place (Belov *et al.*, 2005a; Bombardieri *et al.*, 2007; Plainaki *et al.*, 2007, 2010), a statistical analysis among some of the most intense events could possibly point to their common physical characteristics and contribute in this way to a better understanding of the physics in this field. For this reason, we carried out a statistical analysis of the most intense events occurring during the last Cycles 22 and 23 (1986–2008), using ground-based counting rates. The aim of this work is to provide some evidence for the existence of common physical mechanisms among these events, through the possible similarities of the GLE characteristics. In this work the results for 13 GLE events regarding: *i*) onset-time calculations, *ii*) determination of the maximum cosmic ray intensity and time that it was reached, *iii*) longitudinal and latitudinal distributions, and *iv*) the connection of these events to the current solar activity are presented and discussed. The paper is organized as follows: In Section 2, the data analysis made in this work is presented and discussed analytically. Some specific characteristics of the most intense events of this time period are carefully analyzed in Section 3. In Section 4 our results on the definition of the various GLE parameters are presented and discussed and in Section 5 the main conclusions of this work are summarized.

2. Data Analysis

During solar Cycles 22 and 23, the worldwide neutron-monitor network recorded 31 ground-level enhancements. Fifteen events occurred during the 22nd cycle and 16 events during the
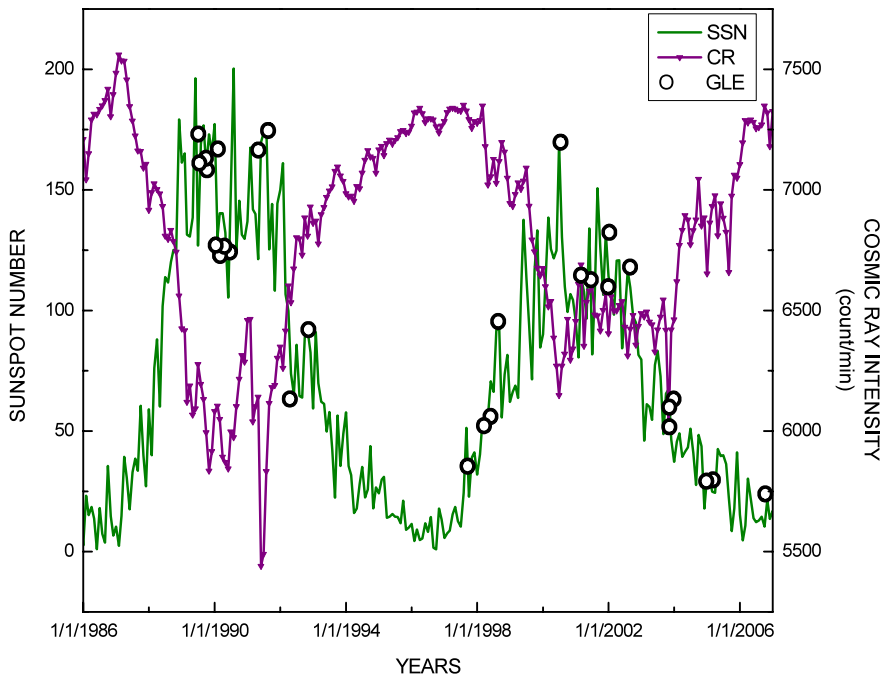
Figure 1 Time evolution of the sunspot number (continuous, green line), the cosmic ray intensity from the Apatity neutron-monitor station (continuous, purple line with triangles) and the GLE appearance (circles) during Cycles 22 and 23.

23rd one. A list of the events can be found in http://neutronm.bartol.udel.edu/~pyle/GLE_List.txt.

The evolution of the number of sunspots together with the cosmic ray intensity as recorded at the Apatity neutron-monitor station during this time period are presented in Figure 1. The anti-correlation between solar activity represented by the sunspot number and the cosmic ray intensity has been shown in the past (Forbush, 1956). The GLE appearance rate during these two Solar Cycles is also illustrated in the figure. Although the majority of the events (11 out of 15 events) that were recorded in the 22nd solar cycle occurred near the cycle's maximum phase and some events were also recorded during the declining phase, the GLE appearance rate in Solar Cycle 23 had a quite unusual behavior. Four GLEs occurred during the rising phase of this cycle, only five events near the maximum phase, while seven more events occurred during the declining phase. Three of them occurred during the period of October–November 2003 (GLE65, GLE66, GLE67) and were associated with an unexpected burst of solar activity (Eroshenko *et al.*, 2004; Plainaki *et al.*, 2005; Uddin, Chandra, and Ali, 2006). The great event of 20 January 2005 (GLE69), which had a comparable intensity with the biggest event ever recorded (*i.e.* the GLE of 23 February 1956 or GLE05), also appeared among these seven events.

An extended study of 13 intense ground-level enhancements of the 22nd and the 23rd solar cycles has been performed. The list of these events together with some special characteristics is given in Table 1. Normalized cosmic ray intensity data of five-minute resolution, and one-minute resolution in some cases, from 48 stations in total of the world-wide neutron-monitor network have been used. In Table 1 the date of each event, the X-ray

Table 1 GLE and flare-associated characteristics using 5-min data.

GLE event	Flare parameters		GLE parameters				
	X-ray class Coordinates	Flare onset-max (UT)	T_{on} (UT)	I_{max} (%)	T_{max} (UT)	$T_{max} - T_{on}$ (min)	NM with I_{max}
GLE42 29/09/1989	X9.8/S26W100	10:47 – 11:33	11:40	403.60	12:55	75	CALG
GLE43 19/10/1989	X13/S27E10	12:29 – 12:45	13:05	91.80	16:35	210	SOPO
GLE44 22/10/1989	X2.9/S27W31	17:08 – 17:57	18:00	155.90	18:05	5	MCMD
GLE45 24/10/1989	X5.7/S30W57	17:36 – 18:31	18:35	202.90	20:35	120	SOPO
GLE48 24/05/1990	X9.3/N33W78	20:46 – 20:49	21:05	49.6	21:15	10	MTWL
GLE52 15/06/1991	X12/N33W69	08:08 – 08:31	08:35	55.80	09:35	60	SOPO
GLE59 14/07/2000	X5.7/N22W07	10:03 – 10:24	10:35	57.80	11:25	50	SOPO
GLE60 15/04/2001	X14.4/S20W85	13:19 – 13:50	14:00	225.40	14:30	30	SOPO
GLE65 28/10/2003	X17.2/S16E08	09:51 – 11:10	11:10	44.70	11:50	40	MCMD
GLE66 29/10/2003	X10/S15W02	20:37 – 20:49	20:35	34.00	22:35	120	SOPO
GLE67 02/11/2003	X8.3/S14W56	17:03 – 17:25	17:30	36.00	17:50	20	SOPO
GLE69 20/01/2005	X7.1/N14W61	06:36 – 07:01	06:30	4809.00	06:50	20	SOPO
GLE70 13/12/2006	X3.4/S06W23	02:14 – 02:40	02:45	92.10	03:05	20	OULU

classification, the coordinates, the onset time and the maximum time of the flare as well as the onset time, the maximum cosmic ray intensity (in percentage above the base level defined one hour prior to the onset of the event), the time the maximum intensity was reached, the time difference between the time of the maximum and the onset time of each GLE, and finally the neutron-monitor station that recorded the maximum cosmic ray intensity using data of 5-min resolution are shown. The same analysis only for the events of the 23rd cycle using 1-min data is given in Table 2 including the GLE parameters and the time difference between the onset times using 5-min and 1-min data. Furthermore, the characteristics of the neutron-monitor stations that were used in this analysis are given in Table 3. The vertical cut-off rigidities of the stations were derived from Shea and Smart (2001). The original neutron-monitor data were collected from the IZMIRAN event database (ftp://cr0.izmiran.rssi.ru/COSRAY!/FTP_GLE/), as well as from the recently created real-time high-resolution Neutron-monitor Database (NMDB) (http://www.nmdb.eu) (Mavromichalaki *et al.*, 2010).

Table 2 GLE characteristics using 1-min data.

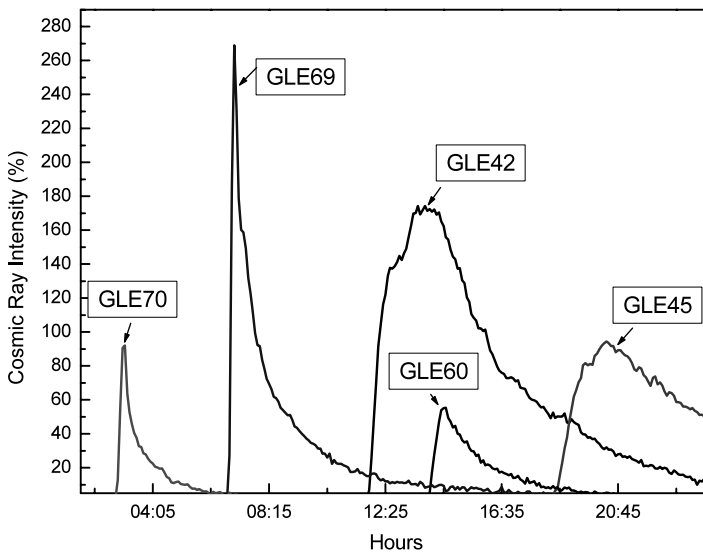| GLE event	T_{on} (UT)	NM with I_{max}	I_{max} (%)	T_{max} (UT)	$T_{max} - T_{on}$ (min)	ΔT_{on} (min)
GLE59 14/07/2000	10:34	SOPO	59.40	11:52	78	1
GLE60 15/04/2001	13:58	SOPO	236.70	14:34	36	2
GLE65 28/10/2003	11:09	MIME	46.90	11:52	36	1
GLE66 29/10/2003	20:32	SOPO	35.20	21:30	58	3
GLE67 02/11/2003	17:29	SOPO	38.60	17:51	22	1
GLE69 20/01/2005	06:30	SOPO	5444.00	06:53	23	0
GLE70 13/12/2006	02:42	OULU	92.00	03:05	24	0

Figure 2 Time profiles of the most intense GLEs during Cycles 22 and 23, as recorded by Oulu neutron-monitor station. The GLEs depicted in the figure are GLE42 (29 September 1989), GLE45 (24 October 1989), GLE60 (15 April 2001), GLE69 (20 January 2005) and GLE70 (13 December 2006).

The most intense GLEs of Cycles 22 and 23, as they were registered at Oulu neutron-monitor station on the basis of 5-min data, are exhibited in Figure 2. Oulu station was selected because: *i*) being a sub-polar station (R_c: 0.77 GV), it usually registers GLEs and *ii*) technically, this neutron-monitor instrument has provided continuous, reliable and accurate data over the whole period of Cycles 22 and 23 (1986 – 2008). According to the

Table 3 Characteristics of neutron-monitor stations used in this analysis (cut-off rigidities derived from Shea and Smart (2001)).

NM Station	Abbrev.	Latitude (deg)	Longitude (deg)	R_c (GV)	Altitude (m)
Alma Ata	AATA	43.25	76.92	6.45	1700
Apatity	APTY	67.55	33.39	0.55	177
Athens	ATHN	37.58	23.47	8.53	260
Baksan	BKSN	43.28	42.69	5.60	1700
Bern	BERN	46.95	7.45	4.42	570
Calgary	CALG	51.08	−114.13	1.09	1128
Cape Schmidt	CAPS	68.92	−179.47	0.52	0
Climax	CLMX	39.37	−106.18	2.93	3400
Deep River	DPRV	46.10	−77.50	1.25	145
Durham	DRHM	43.10	−70.83	1.76	0
Erevan	ERVN	40.28	44.10	7.36	3200
Fort Smith	FRSM	60.02	−112.00	0.30	206
Goose Bay	GSBY	53.27	−60.4	0.74	46
Hermanus	HRMS	−34.25	19.13	4.45	26
Inuvik	INVK	68.40	−133.72	0.14	21
Irkutsk	IRKT	52.28	104.02	3.49	475
Jungfraujoch	JUNG	46.55	7.98	4.59	3570
Jungfraujoch-1	JUN1	46.55	7.98	4.59	3475
Kerguelen	KERG	−49.35	70.27	1.14	33
Kiel	KIEL	54.30	10.10	2.36	54
Kiev	KIEV	50.72	30.30	3.39	120
Kingston	KGSN	−42.99	147.00	1.82	65
Larc	LARC	−62.20	−58.96	3.01	40
Lomnicky Stit	LMKS	49.20	20.22	3.88	2634
McMurdo	MCMD	−77.95	166.60	0.00	48
Magadan	MGDN	60.04	151.05	1.99	220
Mawson	MWSN	−67.60	62.88	0.15	30
Mexico City	MXCO	19.33	−99.18	8.02	2274
Moscow	MOSC	55.47	37.32	2.30	200
Mt Norikura	MTNR	36.11	137.55	11.25	2770
Mt. Washington	MTWS	44.27	−71.30	1.58	1909
Mt Wellington	MTWL	−42.92	147.24	1.83	725
Nain	NAIN	56.55	−61.68	0.45	0
Newark	NWRK	39.70	−75.75	2.21	50
Norilsk	NRLK	69.26	88.05	0.53	0
Novosibirsk	NVBK	54.48	83.00	2.69	163
Oulu	OULU	65.05	25.47	0.77	15
Peawanuck	PWNK	54.98	85.44	0.40	0
Potchefstroom	PTFM	−26.42	27.06	6.85	1351
Rome	ROME	41.86	12.47	6.27	0
Sanae	SNAE	−71.67	−2.85	0.75	856

Table 3 (*Continued*)

NM Station	Abbrev.	Latitude (deg)	Longitude (deg)	R_c (GV)	Altitude (m)
South Pole	SOPO	−90.00	0.00	0.05	2820
Tbilisi	TBLS	41.43	44.48	6.55	510
Terre Adelie	TERA	−66.65	140.00	0.00	32
Thule	THUL	76.50	−68.70	0.00	26
Tixie Bay	TXBY	71.36	128.54	0.43	0
Tsumeb	TSMB	−19.20	17.35	9.06	1240
Yakutsk	YKTK	62.01	129.43	1.55	105

Oulu recordings, the most intense events are (in order of magnitude): GLE69 (20 January 2005), GLE42 (29 September 1989), GLE45 (24 October 1989), GLE70 (13 December 2006) and GLE60 (15 April 2001). In our analysis we noticed that two out of the five most intense events of the two cycles occurred during the declining phase of the 23rd solar cycle. Differences among the time profiles of the five events can be observed in Figure 2. It is noted that the events GLE69, GLE70 and GLE60 were recorded with a sharp and rapid increase in cosmic ray intensity, while the events GLE42 and GLE45 had wider time profiles and less rapid evolvement (*i.e.* they appeared less impulsive). An interesting remark arising from this analysis is that if we compare the flare coordinates with the time profiles of GLE45 and GLE70 we should expect the opposite picture, with the time profile of GLE45 being the sharpest one since its related flare is located near the foot point of the garden hose (Parker spiral) field line (Duldig *et al.*, 1993). The fact that the event GLE45 took place during a medium disturbed condition, $K_p = 4$, should also be taken into consideration for this difference in the profiles, since the direction of the garden hose field line and the foot point at the Sun may vary considerably when the interplanetary conditions deviate from the quiet case (Duldig *et al.*, 1993). More information about the acceleration mechanisms of these events could be deduced after a comparison of the ground-based time profiles of the neutron monitors with observations of electromagnetic radiations from the Sun at different wavelengths (Bütikofer *et al.*, 2009; Masson *et al.*, 2009) but this could be a difficult procedure, especially when the interplanetary conditions are not quiet, as for example in the case of GLE45.

The distribution of the annual solar cosmic ray intensity during solar Cycles 22 and 23 using again the Oulu neutron-monitor data is illustrated in Figure 3. It is shown that the year 1989 was the year with the maximum annual record in the solar cosmic ray intensity. It is important here to note that, due to the anisotropy of ground-level enhancements, if another station were used in this distribution, Figures 2 and 3 would probably be different. Especially, comparing all the available data from the worldwide network of neutron monitors, it is found that the five most intense GLE events are: the event on 20 January 2005 (GLE69), the event on 29 September 1989 (GLE42), the event on 15 April 2001 (GLE60), the event on 24 October 1989 (GLE45), and the event on 22 October 1989 (GLE44) (Table 1). Also, if the recordings from South Pole, McMurdo or Terre Adelie were used in Figure 3, the year 2005 would be the year with the maximum annual solar cosmic ray intensity, having a great difference in comparison to the annual record of the other years. The reason of this difference is the fact that during the event of the 20th January 2005 these three stations recorded a maximum amplitude of the cosmic ray intensity that was greater than 2000% (South Pole 4809%, McMurdo 2093%, Terre Adelie 2650% using 5-minute data), while Oulu station
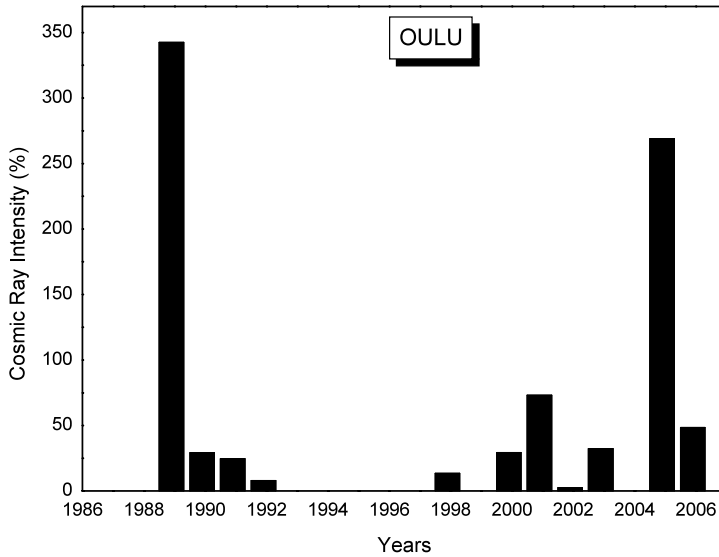
Figure 3 Distribution of the annual Solar cosmic ray intensity during Solar Cycles 22 and 23.

recorded only 269%. It is also noted that if the annual solar cosmic ray intensity for the years 2005 and 2006 were not taken into account, then the distribution of the annual cosmic ray intensity would have a similar evolvement with the sunspot number of Solar Cycles 22 and 23, which is presented in Figure 1.

3. A Short Description of Selected GLE Events

The event of 29 September 1989, also known as GLE42, was the most intense event of the 22nd solar cycle. It occurred shortly after a strong X9.8 X-ray flare and reached a maximum amplitude of 403.6%, which was recorded on the Calgary neutron-monitor station. The event started approximately at 11:40 UT on the ground and some evidence revealed the possibility of the two-peak structure that was reported by Mathews and Venkatesan (1990) and Smart *et al.* (1991). An analysis of this event together with the event of 22 October 1989, which recorded an increase in cosmic ray intensity higher than 150%, can be found in Duldig *et al.* (1993).

Near the maximum solar activity of the 23rd solar cycle an important GLE, the event on 14th July 2000 (GLE59), occurred recording a cosmic ray increase that reached 59.4% at the South Pole station using 1-min data. The event was linked to a N22W07/3B X5.7 flare that occupied an extended area along the solar equator and involved activity in the whole central area on the Sun (Belov *et al.*, 2001). A great disturbance associated with the event led to a deep Forbush decrease (10.7% in 10 GV cosmic rays).

The Easter GLE (or GLE60) (Bombardieri *et al.*, 2007; Plainaki *et al.*, 2010), which is considered to be among the most intense GLE events that were recorded during the Cycles 22 and 23 (see Figure 2), occurred more than 30 minutes after an exceptionally strong X14.4 X-ray flare (S20W85/2B) had been recorded. The spectrum was initially very hard and softened during the declining phase. The event also seems to be associated with a partial halo CME that had a linear velocity of 1199 km sec^{-1}. An extended study of this event
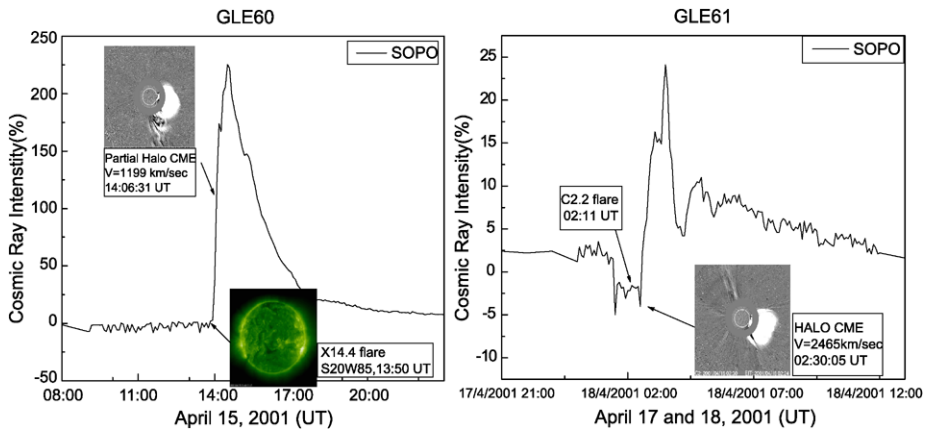
Figure 4 Time profiles of the events of April 2001, as recorded by the South Pole neutron-monitor station. During the event of 18 April, the source region was more than 20 heliographic degrees behind the west limb, and therefore the associated flare was almost entirely occulted.

through the application of the neutron-monitor-based anisotropic GLE model, the NMBAN-GLE PPOLA model, can be found in Plainaki *et al.* (2010). An important anisotropy of the cosmic ray counting rates between the north and the south hemispheres during the initial phase of the event was also recorded. This conclusion was derived from the comparison of the time profiles of Thule (north hemisphere) and McMurdo (south hemisphere) neutron monitors, the choice of which has been explained by Pomerantz and Duggal (1972). An unusual difference was also observed in the time profiles of Oulu and Apatity stations during the event of 15 April 2001. Since Oulu and Apatity are two neutron monitors with very similar characteristics (Oulu long: 25.47°, lat: 65.05°, alt: 15 m, cut-off rigidity R_c: 0.77 GV and Apatity long: 33.39°, lat: 67.55, alt: 177 m, R_c: 0.55 GV) it is expected to record approximately the same rates of cosmic ray intensity increase. However, this was not the case in GLE60; Oulu recorded a 13.2% (using 5-min data) higher maximum increase than Apatity's maximum increase, a fact leading once more to the conclusion that GLE60 was a quite anisotropic event. Differences between the time profiles of these two stations were also noted for the previous GLE events occurring on 2 May 1998 and on 14 July 2000 (Vashenyuk *et al.*, 2001).

Only three days after the occurrence of GLE60 a new event, the event of 18 April 2001 (GLE61), was recorded. This rather weak event seems to be connected with a C2.2 flare that is estimated to have occurred behind the west limb (Belov *et al.*, 2010), so the true X-ray flare importance must have been much higher, and that came with a great halo CME that had a linear velocity of 2465 km sec^{-1}. Comparing the time profiles of the two events, which are presented in Figure 4, it can be clearly observed that GLE61 had a less rapid evolvement in comparison to GLE60. South Pole was the neutron monitor that recorded the maximum intensity for both of these events, with rates of 225.6% for GLE60 and 24.1% for GLE61 using 5-min data, while 237% was recorded for GLE60 and 26% for GLE61 using 1-min data.

During the extreme burst of solar activity in October–November 2003, a series of outstanding events led to the occurrence of three significant ground-level enhancements in a four-day period, 28 October 2003 (GLE65), 29 October 2003 (GLE66), 2 November 2003 (GLE67). The most intense flare that was ever recorded, $\geq$X28.0/3B also occurred during

this period, on the 4th November 2003, but was not associated with a GLE occurrence. A description of these events can be found in Plainaki *et al.* (2005).

On 20 January 2005, when the solar cycle was at its declining phase, one of the greatest solar cosmic ray events was recorded (GLE69), having a cosmic ray increase that was greater than 5000% at some polar stations. Having a very anisotropic nature, this event also presented a two-peak structure (Saiz *et al.*, 2005; Vashenyuk *et al.*, 2006; Plainaki *et al.*, 2007) with the first (additional) peak probably related with the anisotropy of the beam of particles (Plainaki *et al.*, 2007). Also, a very fast CME with velocity of 3242 km sec^{-1} seems to be connected with this event (Gopalswamy, 2006).

Near the end of the 23rd solar cycle, a GLE with greater than 90% cosmic ray recordings occurred on 13 December 2006. This event had a source of anisotropy that was possibly located near the ecliptic plane (Plainaki *et al.*, 2009b).

4. GLE Parameters' Estimation

The extensive analysis of the intense GLE events during the period 1986 – 2008 gave the opportunity to obtain useful results concerning the following GLE parameters.

4.1. Onset Time and Maximum Intensity

Diverse definitions for the GLE onset time have been considered in various works in the past (Tylka *et al.*, 2003; Souvatzoglou *et al.*, 2009). We note that different definitions and calculation methods for the GLE onset are often related to the fact that in certain cases a real-time onset estimation is desired. For example, in order to establish an accurate real-time alert system for the arrival of a GLE event, Souvatzoglou *et al.* (2009) calculated the onset time on the basis of a moving baseline. The calculation of the onset time, T_{on}, of the 13 GLE events for each neutron-monitor station in that case had been carried out using data with 5-min and 1-min resolution where they were available. In the present study, however, an offline data analysis is made. Consequently, the onset time of a GLE event for a specific NM station is defined as the time-lag at which the following two conditions are fulfilled: *i*) the cosmic ray intensity registered at this station obtains a value greater than or equal to $\langle I \rangle + 2\sigma$, where $\langle I \rangle$ is the % mean cosmic ray intensity over a 'background' period and σ is the standard deviation, and *ii*) a period of at least three continuous time lags corresponding to cosmic ray intensity measurements greater than or equal to $\langle I \rangle + 2\sigma$ begins. We point out that the 'background' period is selected as the 1-hour period before the occurrence of the event. Slight differences in the results of 5-min and 1-min data calculations appear in Tables 1 and 2. Additionally, a calculation of the onset-time variability for each GLE among all the neutron monitors that observed a GLE event has been realized. Using the best resolution available, it was found that in 12 out of the 13 GLE cases studied an onset-time variability was present, ranging from 10 to 35 minutes, meaning that NM stations responded to the events with phase differences. The event of 29 October 2003 was the exception, having an onset-time variability of 75 minutes. This event was, of course, very complicated due to the magnetospheric effect that was also recorded on the same day and seems to have affected the evolution of the GLE event (Plainaki *et al.*, 2005; Belov *et al.*, 2010).

Furthermore, the identification of the maximum intensity rate, the time that the maximum flux was recorded as well as the time-lag between the time of the maximum amplitude and the onset time are realized using both 5-min and 1-min data, where this was possible, for each station and for each GLE that was included in this analysis. The main results of this
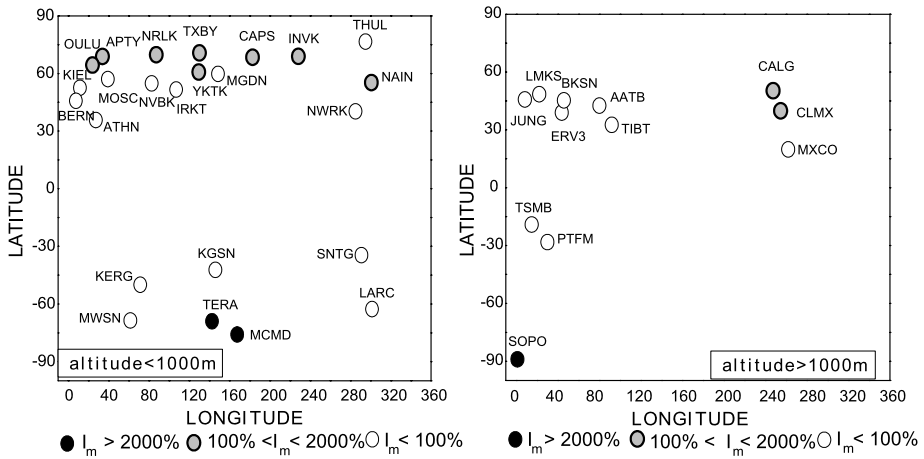
Figure 5 Latitudinal and longitudinal distributions of GLE69 in different NM stations with altitude < 1000 m (left panel) and altitude > 1000 m (right panel).

analysis for the stations that recorded the maximum amplitude for each GLE are exhibited in Table 1.

We find that in all the examined cases the GLE onsets that were calculated using data with 1-min resolution are registered earlier (from 0 to 3 minutes) compared to the onsets calculated using 5-min data. Provided that these high-resolution data are reliable enough, we conclude that 1-min resolution data are of crucial importance when it comes to the GLE-alert calculation. As far as the maximum intensity calculation is considered, an increase in the amplitudes of 1-min data from approximately 1% up to more than 600% was recorded in the examined cases. Also in five out of the six examined cases the time that the maximum was recorded (T_{max}) has a time delay from 1 to 27 minutes when 1-min data were used. Specific conclusions could not be made for the $T_{max} - T_{on}$ parameter, since the differences (while using 1-min or 5-min data) in the calculation of this parameter are extremely variable. We conclude, however, that, using 1-min data, additional information concerning the evolution of a GLE event can be obtained. It should also be noted that calculations using 1-min data were realized in this study only for the events of the 23rd cycle, since there was a very limited number of 1-min data for Solar Cycle 22. The fact that some neutron-monitor stations were out of use, whereas some others began to function only during this 21-year period, also constitutes a problem for a good statistical analysis. Therefore, the importance of a common database that includes a complete set of accurate data with the best resolution, such as the NMDB database (http://www.nmdb.eu), becomes apparent.

4.2. Longitudinal and Latitudinal Distributions

The neutron-monitor stations used here were separated in two categories according to their altitude: stations located at latitude below 1000 m and those with altitude above 1000 m. Two geographical "maps" for each examined GLE event were therefore constructed in an effort to determine if some regions systematically record higher intensity rates. In Figure 5 we present the results of the application of this analysis method to GLE69. The cosmic ray intensity at the maximum of the event, I_m, is divided into three different intensity ranges in order to obtain a clear picture: i) higher, *i.e.* greater than 2000%, ii) medium, *i.e.* lower than

2000% and greater than 100% and *iii*) lower, *i.e.* lower than 100%. We find that NM stations that are located at two specific geographical regions, *i*) and *ii*), record in the most cases the highest cosmic ray intensity rates. These two regions are:

- *i*) with longitude from 0° to 167° and latitude from −90° to −43°,
- *ii*) with longitude from 150° to 300° and latitude from 43° to 77°.

Moreover, the maximum intensity recorded for each GLE is usually recorded inside these regions. On the other hand, two regions, the first with longitude from 18° to 28° and latitude from −35° to 19° and the second with longitude from 7° to 105° and latitude from 40° to 61°, seem to record the lowest rates of intensity. There are many cases in which stations from these areas cannot record a GLE due to the anisotropic nature of the event. These results are of course dependent on rigidity and therefore on latitude, while the altitude of the stations always plays an important role, since neutron-monitor stations at high altitudes always record higher rates compared to other neutron-monitor stations at low altitudes and with similar characteristics.

Unfortunately, an exact determination of these regions and a mean intensity rate at each region cannot be provided at present, since neutron monitors do not exist at every geographical region and furthermore, some neutron monitors were in operation only during a few events. Also, due to the anisotropy of these events, it is normal to detect differences in these regions during the different solar energetic particle events.

4.3. Solar Activity

Finally, the solar and geomagnetic activity that seems to be connected with the GLE occurrence has been examined. Specifically, available data from the solar flares, the coronal mass ejections, the sudden storm commencements and the index of geomagnetic activity Dst near the period of the GLE occurrence have been collected, studied and compared. Unfortunately, there were no CME data available for almost the whole period of the 22nd solar cycle.

From this analysis it is derived that all the examined GLE events, and consequently all the intense events of the 22nd and the 23rd solar cycle, seem to be associated with X-ray solar flares of class X with a mean value X9.1. This is higher than the mean value that includes all the 31 events, which was X6.8 (excluding the C9.7 and the C2.2 flares that were connected with the events of 28 May 1990 and 18 April 2001, respectively, and that were occulted). The X-ray flares related to the events of the 22nd solar cycle seem to be slightly more intense (mean value for all the events of Solar Cycle 22: X7.9 and ranging from X1.4 to X20) compared to those related to the events of the 23rd solar cycle (mean value for all the events of solar Cycle 23: X5.9 and ranging from M7.1 to X17.2). It is also concluded that the GLE events are not necessarily associated with the most energetic solar flares that occur in a cycle. As an example, the mega flare ≤X28.0, which occurred on the 4th November 2003 and is the most intense flare ever recorded, is somehow not connected with a GLE appearance.

Also, the 85% of the GLE related flares originate from a west position, in agreement with previous results (Duldig, 1994; Belov *et al.*, 2010); it can be explained on the basis of the typical geometry of the "garden hose" (Parker spiral) field line that connects the Sun to the Earth. The 63.6% of the western flares also had a south hemispheric origin, while the rest, 36.3%, originated from the north. Furthermore, the events of the 23rd solar cycle seem to be connected with either halo or partial halo CMEs having plane-of-the-sky speeds (POS; with linear fitting) from 1054 km sec^{-1} up to 3424 km sec^{-1}.

5. Discussion and Conclusions

After analyzing separately the properties of every one of the 13 intense GLE events appearing in Solar Cycles 22 and 23, a comparison among them was realized and some significant results of this analysis are summarized below.

1. Solar Cycles 22 and 23 were characterized by an intense solar activity. A great number of GLE events in both of them has been observed, but with an unusual distribution especially for the case of Solar Cycle 23. While in Cycle 22 most events appeared during the maximum, in Cycle 23 most events took place during the declining phase. Also, the GLEs of Cycle 22 seem to be associated with slightly more energetic solar flares.
2. Very intense X-ray flares are not necessarily the ones that produce the most intense GLEs. However, great flares with no GLE (*e.g.* the X-ray flare $\geq$X28.0 with heliocoordinates S19W83, which was recorded on 4 November 2003) do exist in the period studied. The position of the flare seems to play a key role. 85% of the X-ray solar flares of class X that are possibly connected with GLE production originate from west, while 64% of them originate also from a south hemispheric solar active region. The mean X-class value for the X-ray flares associated with the GLE events is X9.1.
3. All GLEs of the 23rd solar cycle seem to be associated with a halo or a partial halo CME with a mean POS (linear) velocity 1932 km sec^{-1}. Only few available CME data existed during Cycle 22.
4. Two geographical regions that are defined approximately from the neutron-monitor recordings, region 1: long.: 0° to 167°, lat.: −90° to −43° and region 2: long.: 150° to 300°, lat.: 43° to 77°, seem to record the highest rates of cosmic ray intensity. The maximum intensity of each event usually occurs in one of these areas. These results depend on rigidity and altitude and may vary due to the anisotropic nature of the GLE events.
5. An onset-time variability of at least 10 minutes among all neutron monitors that recorded a GLE event was noted. Some events, like GLE43 and GLE69, had anisotropic onset times (35 minutes), while the very complicated event GLE66 had a 75-minute onset-time variability. Onset calculations using 1-minute data that are necessary for more accurate onset-time calculations were only possible for the events that occurred during the 23rd solar cycle.

Finally, it is concluded that the existence of accurate data in a common format from all the neutron monitors stations of the worldwide network is of major importance for carrying out a more precise statistical analysis or for studying separately future events. The high-resolution neutron-monitor database NMDB was recently created with this goal in mind and will give the opportunity for a more extended analysis of cosmic ray events in the future.

References

Belov, A., Bieber, J.W., Eroshenko, E.A., Evenson, P., Gvozdevsky, B.B., Pchelkin, V.V., Pyle, R., Vashenyuk, E.V., Yanke, V.G.: 2001, In: *Proc. 27th Int. Cosmic Ray Conf.*, 3446.

Belov, A., Eroshenko, E., Mavromichalaki, H., Plainaki, C., Yanke, V.: 2005a, *Ann. Geophys.* **23**, 2281.

Belov, A., Eroshenko, E., Mavromichalaki, H., Plainaki, C., Yanke, V.: 2005b, *Adv. Space Res.* **35**(4), 697.

Belov, A., Eroshenko, E., Mavromichalaki, H., Plainaki, C., Yanke, V.: 2005c, In: *Proc. 29th Int. Cosmic Ray Conf.* **1**, 189.

Belov, A., Eroshenko, E., Kryakunova, O.N., Kurt, V.G., Yanke, V.G.: 2010, *Geomagn. Aeron.* **50**, 21.

Bombardieri, D.J., Michael, K.J., Duldig, M.L., Humble, J.E.: 2007, *Astrophys. J.* **665**, 813.

Bütikofer, R., Flückiger, E.O., Desorgher, L., Moser, M.R., Pirard, B.: 2009, *Adv. Space Res.* **43**, 499.

Cramp, J.L., Duldig, M.L., Flückiger, E.O., Humble, J.E., Shea, M.A., Smart, D.: 1997, *J. Geophys. Res.* **102**(A11), 24 237.

Dorman, L., Pustil'nik, L.A., Sternlieb, A., Zukerman, G.: 2003, *Adv. Space Res.* **31**, 847.

Duldig, M.L.: 1994, *Proc. Astron. Soc. Aust.* **11**(2), 110.

Duldig, M.L., Cramp, J.L., Humble, J.E., Smart, D.F., Shea, M.A., Bieber, J.W., Evenson, P., Fenton, K.B., Fenton, A.G., Bendoricchio, M.B.M.: 1993, *Proc. Astron. Soc. Aust.* **10**(3), 211.

Eroshenko, E., Belov, A., Mavromichalaki, H., Mariatos, G., Oleneva, V., Plainaki, C., Yanke, V.: 2004, *Solar Phys.* **224**, 345.

Flückiger, E.O., Bütikofer, R., Desorgher, L., Moser, M.R.: 2006, In: *36th COSPAR Scientific Assembly*, 3042.

Forbush, S.E.: 1956, *J. Geophys. Res.* **61**(1), 155.

Gopalswamy, N.: 2006, *J. Astrophys. Astron.* **27**(2), 243.

Humble, J.E., Duldig, M.L., Shea, M.A., Smart, D.F.: 1991, *Geophys. Res. Lett.* **18**, 737.

Masson, S., Klein, K.L., Bütikofer, R., Flückiger, E.O., Kurt, V., Yuskov, B., Krucker, S.: 2009, *Solar Phys.* **257**, 305.

Mathews, T., Venkatesan, D.: 1990, *Nature* **345**, 600.

Mavromichalaki, H., Plainaki, C., Gerontidou, M., Sarlanis, C., Souvatzoglou, G., Mariatos, G., Belov, A., Eroshenko, E., Klepach, E., Yanke, V.: 2007, *IEEE Trans. Nucl. Sci.* **54**(4), 1082.

Mavromichalaki, H., Papaioannou, A., Plainaki, C., *et al.* for the NMDB team: 2010, *Adv. Space Res.* doi:10.1016/j.asr.2010.02.019.

Plainaki, C., Belov, A., Eroshenko, E., Kurt, V., Mavromichalaki, H., Yanke, V.: 2005, *Adv. Space Res.* **35**, 691.

Plainaki, C., Belov, A., Eroshenko, E., Mavromichalaki, H., Yanke, V.: 2007, *J. Geophys. Res. A* **112**, 4102.

Plainaki, C., Mavromichalaki, H., Belov, A., Eroshenko, E., Yanke, V.: 2009a, *Adv. Space Res.* **43**(4), 474.

Plainaki, C., Mavromichalaki, H., Belov, A., Eroshenko, E., Yanke, V.: 2009b, *Adv. Space Res.* **43**(4), 518.

Plainaki, C., Mavromichalaki, H., Belov, A., Eroshenko, E., Andriopoulou, M., Yanke, V.: 2010, *Solar Phys.* **264**, 239.

Pomerantz, M.A., Duggal, S.P.: 1972, *J. Geophys. Res.* **77**, 263.

Saiz, A., Ruffolo, D., Rujiwarodom, M., Bieber, J., Clem, C., Evenson, P., Pyle, R., Duldig, M., Humble, J.: 2005, In: *Proc. 29th Int. Cosmic Ray Conf.* **1**, 229.

Shea, M.A., Smart, D.F.: 1982, *Space Sci. Rev.* **32**, 251.

Shea, M.A., Smart, D.F.: 2001, In: *Proc. 27th Int. Cosmic Ray Conf.*, 4063.

Simpson, J.A.: 2000, *Space Sci. Rev.* **93**, 11.

Smart, D.F., Shea, M.A., Taskanen, P.J.: 1971, In: *Proc. 12th Int. Cosmic Ray Conf.* **2**, 483.

Smart, D.F., Shea, M.A., Wilson, M.D., Gentile, L.C.: 1991, In: *Proc. 22nd Int. Cosmic Ray Conf.* **3**, 97.

Souvatzoglou, G., Mavromichalaki, H., Sarlanis, C., Mariatos, G., Belov, A., Eroshenko, E., Yanke, V.: 2009, *Adv. Space Res.* **43**(4), 728.

Tylka, A.J., Cohen, C.M.S., Dietrich, W.F., Krucker, S., McGuire, R.E., Mewaldt, R.A., Ng, C.K., Reames, D.V., Share, G.H.: 2003, In: *Proc. 28th Int. Cosmic Ray Conf.* **6**, 3305.

Uddin, W., Chandra, R., Ali, S.S.: 2006, *J. Astrophys. Astron.* **27**, 267.

Vashenyuk, E.V., Phelkin, V.V., Gvozdevsky, B.B., Usoskin, I.G., Mursula, K., Kovaltsov, G.A.: 2001, In: *Proc. 27th Int. Cosmic Ray Conf.*, 3383.

Vashenyuk, E.V., Balabin, Y.V., Gvozdevsky, B.B., Karpov, S.N.: 2006, *Geomagn. Aeron.* **46**(4), 424.

Wang, R., Wang, J.: 2006, *Adv. Space Res.* **38**(3), 489.